Journal of Alloys and Compounds 743 (2018) 691–696

Contents lists available at ScienceDirect

Journal of Alloys and Compounds

journal homepage: http://www.elsevier.com/locate/jalcom

Controlled hydrogen release from metastable hydrides

Jason Graetz*, John J. Vajo

HRL Laboratories, LLC, 3011 Malibu Canyon Road, Malibu, CA 90265, USA

ARTICLE INFO

Article history:
Received 7 December 2017
Received in revised form
26 January 2018
Accepted 30 January 2018
Available online 5 February 2018

Keywords:
Metal hydride
Hydrogen storage
Metastable hydride
Aluminum hydride

ABSTRACT

Metastable hydrides are an interesting class of hydrogen carrier since many offer high volumetric and gravimetric hydrogen densities and rapid hydrogen release rates at low temperatures. Unlike reversible metal hydrides, which operate near equilibrium, metastable hydrogen carriers rely on kinetic barriers to limit or prevent the release of hydrogen and can be prepared in a stabilized state far from equilibrium. Despite the advantage of low temperature hydrogen release, this type of one-way thermolysis reaction can be difficult to control since the hydrogen release rate varies with temperature and composition. Here we developed a kinetic rate equation from a series of isothermal measurements, which describes the relationship between temperature, hydrogen release rate and composition for aluminum hydride. This equation is necessary to thermally control the rate of hydrogen release throughout decomposition. This equation was used to run a fuel cell at a controlled rate of ~1 wt%/hr. Although the equation established in this paper relates specifically to aluminum hydride, the method used is applicable to other metastable hydrides.

© 2018 Elsevier B.V. All rights reserved.

1. Introduction

Hydrogen is a versatile fuel that can easily be converted into useful energy, either through combustion (e.g., internal combustion engine) or through a fuel cell where it can be used to generate electricity for portable electronics, vehicles or stationary applications. However, the challenge of hydrogen storage continues to limit the widespread use of hydrogen, especially at the small and medium scales (e.g., << 1 kg H_2) where high pressure or cryogenic systems become less practical. Metal hydrides may provide a solution to hydrogen storage since they exhibit high volumetric hydrogen densities (2x the density of liquid hydrogen) and are reasonably scalable since they often uptake and release hydrogen under moderate temperatures and pressures.

The release of hydrogen from a metal hydride can be initiated through a variety of methods, the most common of which is a thermolysis reaction (temperature stimulated hydrogen release), where the temperature of the hydride is raised above the equilibrium temperature for a given hydrogen partial pressure. Conversely, hydrogen uptake occurs when the temperature is lowered below the equilibrium temperature for a given partial pressure. In this scenario, the rate of hydrogen release is naturally controlled by a material maintained near equilibrium at a constant temperature.

Hydrogen can also be released from hydrides in metastable states [1]. Under these conditions hydrogen release occurs at pressures much less than the equilibrium pressure (for a given temperature). Equivalently, the temperature required for a practical rate of hydrogen release is much higher than the equilibrium temperature corresponding to a chosen release pressure. For these materials, hydrogen release is controlled by temperature and is largely unaffected by the hydrogen pressure. Metastability originates from kinetic barriers that limit the rate of hydrogen evolution, which, are dependent upon a variety of parameters including availability of nucleation sites, grain boundaries, defects, surface area, thermal conductivity, etc. Generally, a single rate-limiting step can be identified that defines the reaction rate, which, due to its Arrhenius behavior, can be used to thermally control the hydrogen release rate.

As an example, α-AlH_3, is thermodynamically unstable at room temperature and has an equilibrium pressure of around 7 kbar [2,3]. Despite the large driving force for decomposition, the material is easily prepared in a kinetically stabilized state through the formation of a surface oxide/hydroxide layer. This passivation layer prevents H-H recombination at the surface and inhibits decomposition [4,5].

A more quantitative description of a metastable hydride (or metastability) may be established (approximately) by considering

* Corresponding author.
E-mail address: jagraetz@hrl.com (J. Graetz).

https://doi.org/10.1016/j.jallcom.2018.01.390
0925-8388/© 2018 Elsevier B.V. All rights reserved.

the free energy (ΔG) under the conditions where hydrogen is released. In an ideal system with no kinetic limitations, hydrogen release occurs at $\Delta G = 0$, although practically, reversible equilibrium conditions (with no kinetic barrier) are never achieved. For hydrides conventionally referred to as operating under "equilibrium conditions", the ratio of equilibrium pressures (P_{eq}, where $\Delta G = 0$) to desorption pressures (P_d, pressure at which hydrogen is released), is typically $P_{eq}/P_d = \sim 1.05$ to 4 (see details in the supplemental information). This ratio corresponds to $\Delta G = -0.1$ to -4 kJ/mol-H_2 (using -RT•ln[P_{eq}/P_d]) for a desorption temperature of 50 °C (323 K). Hydrides considered to exhibit a metastable character typically have an overpressure of $P_{eq}/P_d \geq 10$, which corresponds to $\Delta G \leq -6$ kJ/mol-H_2 at 50 °C. Thus, approximately, we consider the transition from equilibrium hydrogen release to metastable release to occur at $\Delta G \cong -5$ kJ/mol-H_2.

Examples of metastable hydrides with intrinsic kinetic barriers for hydrogen release include aluminum hydride (alane, AlH_3) [6], lithium aluminum hydride ($LiAlH_4$ and Li_3AlH_6) [7,8] and magnesium aluminum hydride ($Mg(AlH_4)_2$) [9]. For AlH_3 with a desorption enthalpy of $\Delta H = 7.5$ kJ/mol-H_2 and an entropy of 130 J/K-mol-H_2, the equilibrium pressure is 1 bar at −215 °C (58 K). However, hydrogen release at practical rates occurs at temperatures of at least 50 °C, depending on the specific formulation. Under these conditions, $\Delta G = -34.5$ kJ/mol-H_2, clearly illustrating metastable behavior.

In addition to rapid H_2 evolution rates at low temperature (80–100 °C), the low desorption enthalpy means that less heat is required to release the hydrogen at practical pressures. This is especially important for smaller systems (<1 kW) where it may be difficult or impractical to capture waste heat from the fuel cell. In these systems, the enthalpy required for desorption must be supplied by the fuel cell (or combustion of a small amount of the hydride fuel) lowering the overall efficiency of the system. As an example, in a system with no waste heat recovery, ~6% of the energy within α-AlH_3 is required to release the H_2, while as much as 33% of the energy may be consumed for a reversible hydride, such as $NaAlH_4$ (see details in the supplemental information).

Metastable hydrides can also include destabilized (or reactive composite) multiple-phase hydride systems [10,11]. The multiple phases that characterize these systems often impose severe kinetic barriers because these phases must nucleate, grow, and be consumed across solid-solid interfaces during hydrogen exchange. An example is $2MgH_2 + Si$ [12]. For this destabilized system, despite considerable effort, hydrogen release does not begin at practical rates until ~200 °C, at which $\Delta G = -24$ kJ/mol-H_2 (calculation performed using HSC chemistry, version 7.11).

A number of well-known reversible hydrides that can operate near equilibrium in the catalyzed state, may also be considered as metastable hydrides in the uncatalyzed state. In pure, uncatalyzed form, these hydrides often exhibit large kinetic barriers which necessitate high desorption temperatures that push the system far from equilibrium. An example is $NaAlH_4$, which has been thoroughly studied in recent years [13]. Pure bulk $NaAlH_4$ does not begin to release hydrogen until melting, at ~180 °C. At this temperature, $\Delta G = -19$ kJ/mol-H_2. Thus, in pure form, $NaAlH_4$ may be considered a metastable hydride given that it is typically decomposed at a high temperature, far from equilibrium. However, when effectively catalyzed, the release temperature can be lowered considerably and near equilibrium behavior is possible.

To summarize, metastable hydrogen release occurs when the free energy is more negative than ~ -5 kJ/mol-H_2. This kinetically limited condition can occur 1) intrinsically in low enthalpy hydrides, 2) in multiple-phase hydride systems or 3) in hydrides requiring processing to reduce kinetic barriers.

The metastable hydrides may be ideally suited for small portable power systems and unmanned aerial vehicles (UAVs) where weight and volume are critical. A metastable hydride, such as AlH_3, coupled to a proton exchange membrane (PEM) fuel cell could exhibit an energy density substantially larger than even the best batteries currently available (Fig. 1). To estimate the energy density and specific energy of an AlH_3 + PEM fuel cell system we consider that a 10 wt% hydride, such as AlH_3, has a theoretical specific energy of 3.33 kWh/kg and energy density of 4.96 kWh/L, based on the lower heating value of hydrogen. Assuming a practical hydrogen concentration of 9 wt% and including the weight-penalty associated with a thin-walled aluminum tank with an internal heater, we expect a practical specific energy of 2.66 kWh/kg (system, not including fuel cell). Similarly, we estimate a packing density of 60% and an additional 20% loss associated with the volume of the tank, giving an energy density of 2.38 kWh/L (system, not including fuel cell). If we assume a fuel cell efficiency of 60%, and a volume and weight penalty associated with the fuel cell of 20% and 37%, respectively, then we have a system with 1 kWh/kg and 1.14 kWh/L (see supplemental section for additional details). Even under this rather conservative scenario, a hydrogen fuel cell using AlH_3 yields 4 times the specific energy and more than 3 times the energy density of even the best performing lithium batteries. In addition, when compared with state-of-the art hydrogen storage (liquid hydrogen and 700 bar compressed gas), an alane-base system has a comparable specific energy with an energy density that is 2x greater. This comparison (Fig. 1) is based on large scale tanks (>= 1 kg of H_2). Since liquid hydrogen and high pressure compressed gas systems scale poorly as the tank size gets smaller (<1 kg H_2), the advantages of an alane-based system (which is essentially scale independent) increases with decreasing tank size. This is clearly illustrated in Fig. 2, which shows a number of commercially available carbon fiber tanks (200–700 bar) of various sizes and how the hydrogen density compares with an AlH_3-based system. The AlH_3-based PEM fuel cell system is consistently higher in specific energy, but the greatest difference is below ~1 kg H_2 (11,000 standard liters), indicating this system is ideally suited for small-medium sized devices, such as portable power and UAV systems where the total stored energy is ~33 kWh or less.

A system that relies exclusively on hydrogen generated from a metastable hydride requires careful control over the hydrogen release rate so that hydrogen is generated at a rate appropriate for the real-time demand from the fuel cell. This can be a challenge

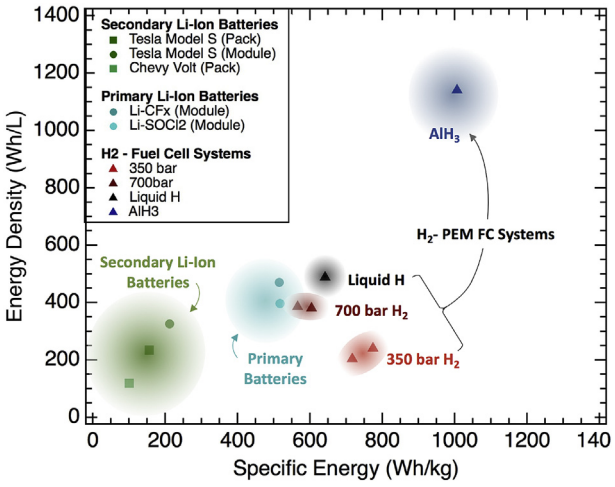

Fig. 1. Plot showing energy density and specific energy for a variety of energy storage systems. The estimates shown were made consistently for complete battery and fuel cell-based systems. Extensive details are given in the supplementary materials section.

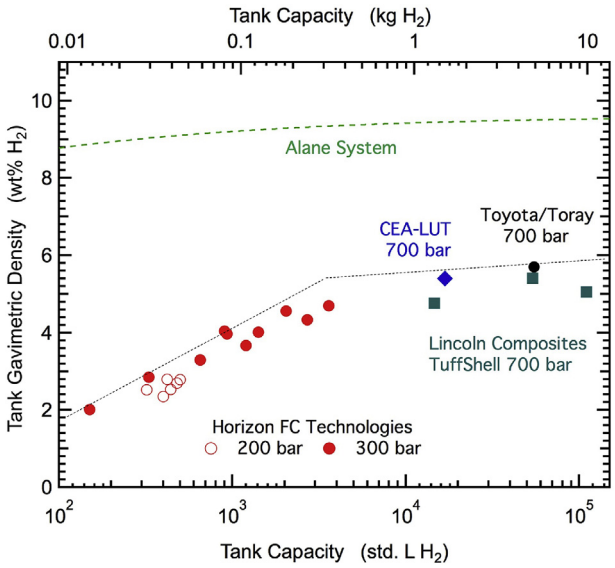

Fig. 2. Gravimetric capacity vs. volume and mass of stored H_2 for a few representative compressed gas tanks (200–700 bar) with a black dotted line representing state-of-the-art. Green dotted line represents an estimate of an alane-based hydrogen storage system. See supplemental information for details. (For interpretation of the references to colour in this figure legend, the reader is referred to the Web version of this article.)

since the hydrogen release rate is not constant with composition (e.g., x in (1-x)AlH_3 + xAl) and, due to the high equilibrium pressure, the flow is not easily turned off. Left unchecked, the hydrogen pressure can become too high, requiring venting to the environment, or fall too low, starving the fuel cell. Accurate control over hydrogen release requires a rate equation, which describes the relationship between H_2 release rate, temperature and composition. Here we establish a method of determining this rate equation and demonstrate the thermal control of hydrogen release using α-AlH_3. However, the approach is general and could be applied to any hydride where heat input is required to remove hydrogen under far from equilibrium conditions, i.e., where the equilibrium hydrogen pressure is much too high for practical applications.

2. Experimental methods and materials

Crystalline α-AlH_3 was prepared by ATK-Thiokol (now Orbital ATK) and obtained from Savannah River National Laboratory. The conventional synthesis of α-AlH_3 involves a reaction between $LiAlH_4$ and $AlCl_3$ in diethyl ether, followed by the removal of LiCl (filtration) to form a solution of alane etherate [3,14]. The final step involves desolvation of the etherate to form the pure crystalline aluminum hydrides. H_2 desorption measurements of the material used in this study indicated a composition of ~8 wt% hydrogen suggesting a purity of ~80% AlH_3 with Al as the most likely impurity (~20%). The 8 wt% hydrogen is likely due to decomposition during storage. The material was stored in an inert Ar glove box, but exhibited slow continuous desorption even at room temperature. Over 2 months of storage at ~25 °C, the hydrogen content decreased from 8 wt% to 7.5 wt%. During 1 year of storage at −30 °C, no further loss of hydrogen was detected.

Isothermal desorption measurements were conducted on 0.3 g AlH_3 loose powder samples using an in-house built Sieverts apparatus that was described previously [12]. Heating to the desired isothermal temperatures was performed at 20 °C/min. An *in-situ* thermocouple inserted into the AlH_3 powder was used for accurate, real-time temperature measurements. The thermocouple was metal sheathed, 1/16 inch OD, and was inserted into the sample vessel through a 1/16 inch bored-through Swagelok fitting. A hydrogen overpressure of ~1.5 bar was also used to improve thermal conductivity within the powder bed and to mimic the conditions when being used as a hydrogen source.

To demonstrate use of AlH_3 as a hydrogen source, a commercially available aluminum canister with a volume of ~10 cm^3 and a screw-on lid was used. The canister was filled with 5 g of tamped AlH_3 powder. An outlet port drilled into the lid contained a 2 μm filter gasket to prevent any entrainment of the AlH_3 in the flowing hydrogen. The canister was heated by heating tape wrapped around the canister which was controlled by a Digi-Sense temperature controller.

The AlH_3 hydrogen source was connected to a 5-stack (~1W) PEM fuel cell from H-Tec. The electrical output from the fuel cell was connected two small fans and a small water pump that provided a constant load. The full set-up is shown in Ref. [15].

3. Results and discussion

3.1. Isothermal desorption and rate equation

Thermal control over hydrogen evolution from a metastable hydride requires a rate equation, which describes the relationship between H_2 release rate, temperature and composition. Here, this equation was determined empirically by: i) collecting a series of isothermal desorption data over the desired temperature (rate) range; ii) fitting those data to a desorption curve to determine a set of coefficients at each temperature; and iii) establishing the temperature relationship of the coefficients.

The results from a series of isothermal decomposition measurements on α-AlH_3 ($AlH_3 \rightarrow Al + 3/2H_2$) are shown in Fig. 3a. In these experiments, approximately 300 mg of α-AlH_3 was sealed in a small reactor and connected to a Sievert's system with a calibrated

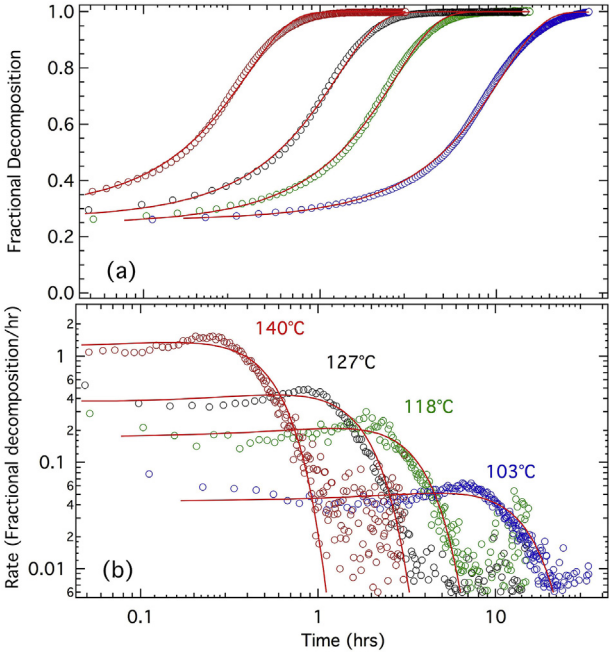

Fig. 3. Isothermal hydrogen desorption from α-AlH_3 (ATK) showing **a**) fractional decomposition and Avrami-Erofeev fit (red solid line) and **b**) the derivative of the fractional decomposition (rate) and the derivative of the fit (red solid line). (For interpretation of the references to colour in this figure legend, the reader is referred to the Web version of this article.)

gas reservoir. The reactor was heated to various temperatures (103 °C–140 °C) using a resistive heating tape and the temperature was monitored with an internal thermocouple. Approximately 7.8 wt % hydrogen was desorbed from these samples with minimal variation from sample-to-sample. Since this material was in a state of partial decomposition (pure AlH_3 contains 10 wt% hydrogen) the maximum evolved hydrogen was uniformly set to 10 wt% (fractional decomposition = 1.0), which more accurately reflects the complete desorption profile for a pure material (i.e., extrapolating back to 0 wt%). The kinetic analysis relies on the fractional decomposition (plotted in Fig. 3) which is simply the amount of evolved hydrogen normalized to 1.0 (all values divided by 10). The rate of hydrogen release was determined from the derivative of the fractional decomposition curve and is shown in Fig. 3b.

The isothermal fractional decomposition curves in Fig. 3a were fit to a modified Avrami-Erofeev equation [16,17], which describes the fractional decomposition as:

$$x(t) = 1 - \exp(-k^n(t+t_0)^n) \tag{1}$$

where t is time, k is the rate constant (function of temperature), n is an exponent determined through the fit (typically 1–3), and t_0 represents the additional time that would be required to decompose the pure hydride from $x = 0$ to $x = 0.215$ (i.e., extrapolating the decomposition curve down to $x = 0$). The best fits were obtained with an exponent of $n = 3$, indicating three-dimensional growth of the Al phase [18]. The curve fits plotted in Fig. 3b represent the rate of hydrogen release, which is the derivative of the fractional decomposition fit, as shown below:

$$r = \frac{dx}{dt} = nk^n(t+t_0)^{n-1}\exp(-k^n(t+t_0)^n) \tag{2}$$

The rate constants and t_0 values determined from the fits in Fig. 3 exhibit an Arrhenius behavior with temperature as shown in Fig. 4. The linear fits to the data plotted in this figure used the following equations for k and t_0:

$$k(\mathrm{T}) = k_0\, exp\left(\frac{-E_a}{RT}\right) \tag{3}$$

$$t_0(\mathrm{T}) = t_{00}\, exp\left(\frac{E_a}{RT}\right) \tag{4}$$

where T is the absolute temperature, R is the gas constant, $k_0 = 2.70 \times 10^{14}$ and $t_{00} = 2.57 \times 10^{-15}$. The activation is energy, E_a, is 113.6 ± 2 kJ/mol H_2, which is similar, but slightly higher (~10%) than previous isothermal desorption measurements for α-AlH_3 [16,17]. Combining Equations (2)–(4) leads to the following equation for the hydrogen release rate:

$$r = nk_0^n\, exp\left(\frac{-nE_a}{RT}\right)\left(t + t_{00}\, exp\left(\frac{E_a}{RT}\right)\right)^{n-1} \exp\left[-k_0^n\, exp\left(\frac{-nE_a}{RT}\right)\left(t + t_{00}\, exp\left(\frac{E_a}{RT}\right)\right)^n\right] \tag{5}$$

Equation (5) describes the relationship between the hydrogen release rate and time for a given temperature. In a real system, it may be necessary to vary the temperature of the metal hydride bed in response to demand from the fuel cell. In this case, it is more useful to describe the hydrogen release rate as a function of temperature and composition, rather than time, as shown in Fig. 5.

The rate of decomposition as a function of composition can be fit using the derivative of the Avrami-Erofeev equation (eq. (2)). Including the Arrhenius parameters (eq. (5)) yields a more complicated expression that describes the rate in terms of temperature and composition. In some cases, it is more useful to invert this expression to describe the temperature necessary to achieve a particular rate at a given composition. In this case, it is simpler to take a more empirical approach and use a standard Lorentzian function to fit the rate vs. composition data shown in Fig. 5:

$$r = r_0 + \frac{A}{(x - x_0)^2 + B} \tag{6}$$

where x is composition and r_0, x_0, A and B are fit parameters. Fits to all four curves exhibited nearly constant values of x_0 and B (average values were $x_0 = 0.577$ and B = 0.267), while r_0 and A exhibited an Arrhenius behavior with temperature:

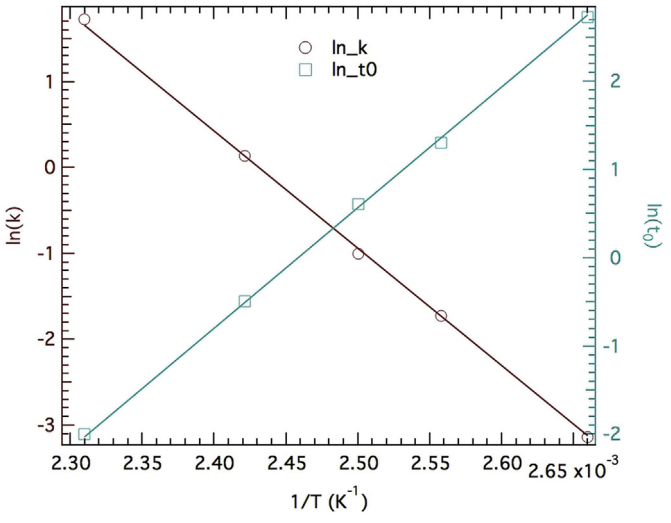

Fig. 4. Arrhenius plot showing ln(k) and ln(t_0) plotted vs. inverse temperature. Values of k and t_0 were determined from the fits in Fig. 3a.

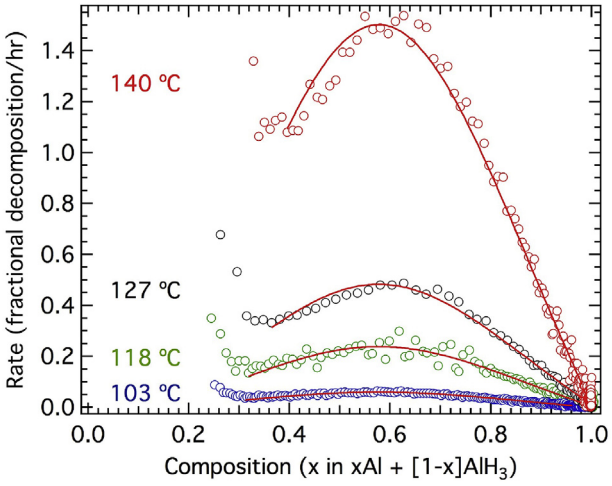

Fig. 5. Isothermal hydrogen desorption from α-AlH_3 (ATK) showing fractional decomposition vs composition. The solid red line represents a fit using a Lorentzian function. (For interpretation of the references to colour in this figure legend, the reader is referred to the Web version of this article.)

$$A(\mathrm{T}) = A_0 exp\left(\frac{-E_a}{RT}\right) \quad (7)$$

$$r_0(\mathrm{T}) = r_{00} exp\left(\frac{-E_a}{RT}\right) \quad (8)$$

Arrhenius plots of ln[$A(T)$] and ln[-$r_0(T)$] as a function of inverse temperature are shown in Fig. 6. Analysis of these plots indicates a common activation energy of 111.2 ± 2 kJ/mol H_2 (similar to that obtained using an Avrami-Erofeev fit). Linear fits using a fixed E_a of 111.2 kJ/mol H_2 provide the following parameters: $A_0 = 1.1 \times 10^{14}$, $r_{00} = -2.49 \times 10^{14}$. Combining equations (6)–(8) gives the following:

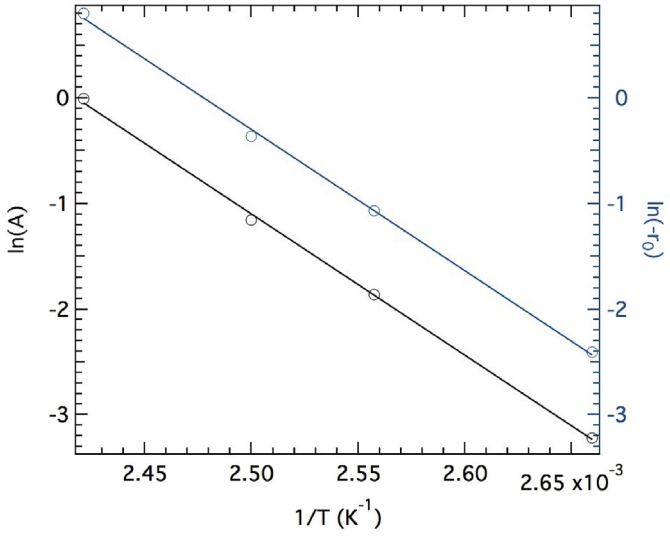

Fig. 6. Fit parameters, ln[$A(T)$] and ln[-$r_0(T)$], plotted as a function of inverse temperature. Solid lines represent linear fits.

$$r = exp\left(\frac{-E_a}{RT}\right)\left(r_{00} + \frac{A_0}{(x - x_0)^2 + B}\right) \quad (9)$$

Rearranging Equation (9) yields an expression for temperature as a function of rate and composition:

$$T = \left[-\frac{R}{E_a} ln\left(\frac{r}{r_{00} + \frac{A_0}{(x-x_0)^2+B}}\right)\right]^{-1} \quad (10)$$

Using Equation (10) we calculated a set of constant rate curves (0.5 wt%/hr, 1 wt%/hr and 2 wt%/hr) as a function of composition (Fig. 7a). Given the rates are constant in these plots it is relatively simple to convert composition into time to get a plot of temperature vs time (Fig. 7b).

The rate equation listed above (eq. (10)) can be used to control the rate of hydrogen release by controlling the temperature of the hydride. Although the curves shown in Fig. 7 correspond to constant rate scenarios, the rate equation can just as easily be used in applications where the rate varies with time. Therefore, this equation could be incorporated into an onboard "hydride management system", which would track hydride composition (x) using flow rate and control the temperature of a hydride bed, or a reactor zone, to provide the appropriate hydrogen release rates to a fuel cell in response to a variable load.

3.2. Demonstration of controlled hydrogen release

To demonstrate the rate equation (eq. (10)) can be used to control the hydrogen release rate, a 300 mg sample of AlH_3 was decomposed using a temperature profile set for 1 wt %/hr (similar to the black curve in Fig. 7). The results of this test are shown in Fig. 8, which show the total evolved hydrogen increases nearly linearly with time at a rate of ~1 wt%/hr.

The previous example demonstrated that a constant hydrogen evolution rate can be obtained from AlH_3 using the derived rate equation (eq. (10)). In the next example a similar temperature profile was used with a 5 g sample of AlH_3 connected to a 5-stack PEM fuel cell. In this example, a constant load was connected to the fuel cell designed to draw a hydrogen flow rate of ~10 sccm. The

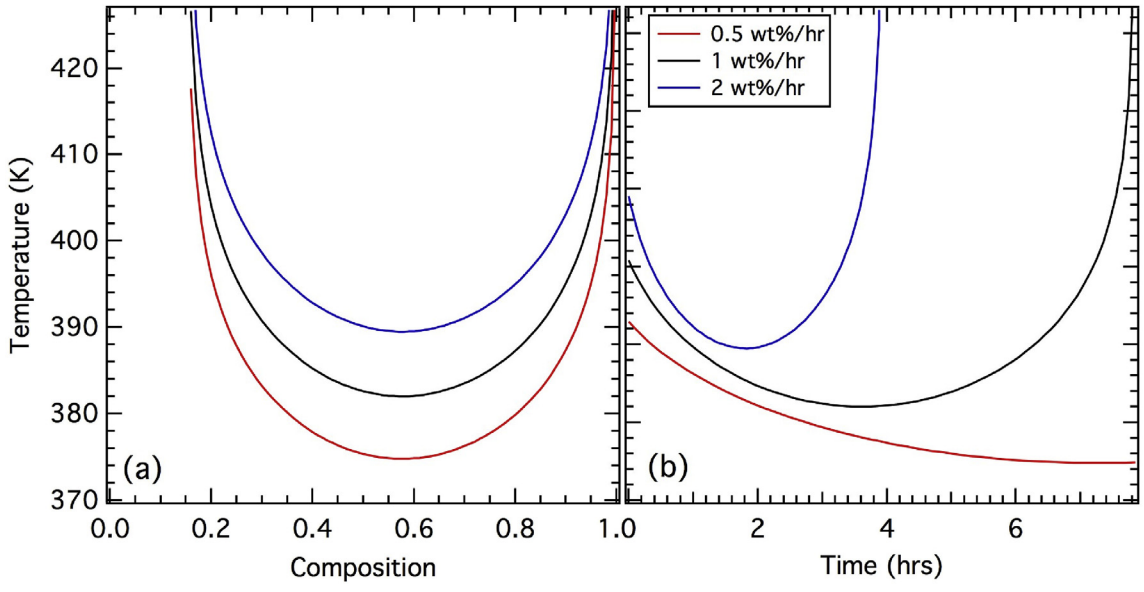

Fig. 7. Constant rate curves (0.5 wt%/hr, 1 wt%/hr and 2 wt%/hr) calculated using equation (10) plotted vs. composition (a) and time (b).

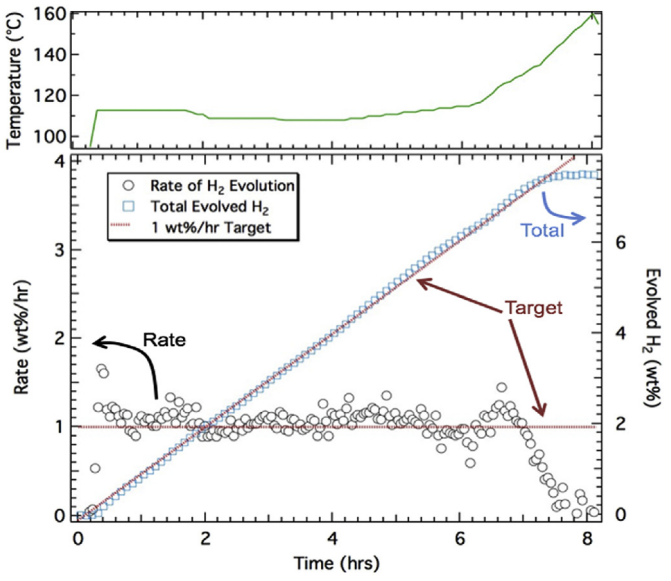

Fig. 8. (bottom) Plot of hydrogen release rate (black) and total amount of hydrogen evolved (blue) along with the targets (red) used in the rate equation. (top) Temperature profile used to achieve the target desorption rate of 1 wt%/hr as determined from eq. (10). (For interpretation of the references to colour in this figure legend, the reader is referred to the Web version of this article.)

hydrogen was supplied from a cartridge of AlH_3 equipped with an internal thermocouple and an external heater. Fig. 9 shows the results from this test. The AlH_3 cartridge supplied a consistent hydrogen flow and nearly constant pressure for ~7 h. The lower plot shows the electrical properties were also reasonably constant over the course of the experiment with the voltage at ~3.2 V, the current at ~200 mA and a power of ~0.8 W. There was no observed degradation in the fuel cell performance after 7 h, indicating little-to-no impurities were entrained in the gas stream. Additional

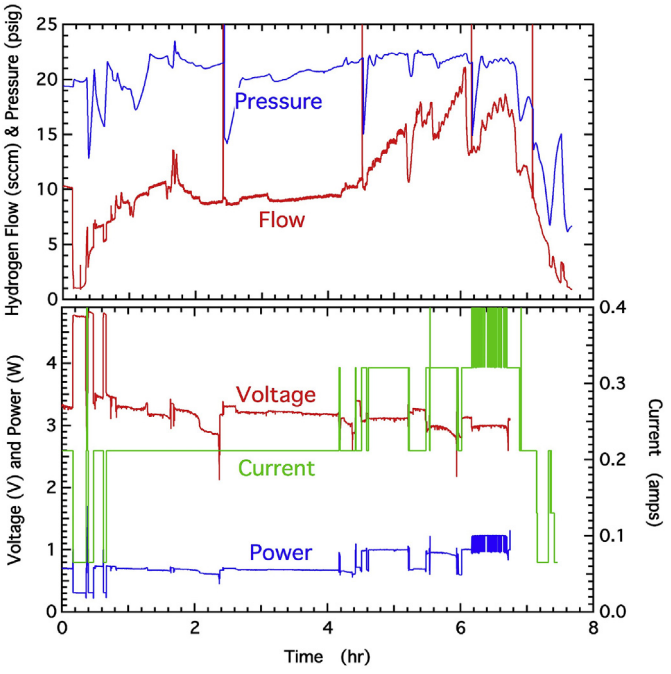

Fig. 9. Results from demonstration with 5 g of AlH_3 connected to PEM fuel cell showing (top) pressure and flow rate along with (bottom) current voltage and power output from the fuel cell over the course of ~7h.

demonstrations were performed with a larger 30 W fuel cell and a cartridge containing 10 g of AlH_3, which was discharged over 20 min. These demonstrations confirm that the established rate equation can be used to thermally control hydrogen release across a spectrum of hydrogen rates (1–20 wt%/hr). On a material basis, these measurements provide a demonstrated (not theoretical) energy density of ~1100 Wh/kg.

4. Conclusion

Metastable hydrides offer high hydrogen densities with low desorption temperatures. However, these hydrides undergo desorption far from equilibrium, making the hydrogen release rates difficult to control. Thermally controlled hydrogen release can be achieved by taking advantage of the natural kinetic barriers present in these systems. This type of controlled thermolysis requires a rate equation, which describes the temperature necessary to achieve a desired hydrogen release rate at a given composition. This rate equation was derived for α-AlH_3, using a series of isothermal desorption measurements which were empirically fit to determine a set of temperature-dependent coefficients. These coefficients exhibit an Arrhenius behavior with temperature with an activation energy of ~111 kJ/mol H_2. Controlled hydrogen release was demonstrated using a 5 g cartridge of α-AlH_3 and a PEM fuel cell, which provided ~0.8 W of power for 7 h, resulting in a specific energy of 1.1 kWh/kg.

Acknowledgements

We gratefully acknowledge Scott McWhorter, Ted Motyka and Ragaiy Zidan at Savannah River National Laboratory for supplying the aluminum hydride.

Appendix A. Supplementary data

Supplementary data related to this article can be found at https://doi.org/10.1016/j.jallcom.2018.01.390.

References

[1] J. Graetz, J.J. Reilly, Scripta Mater. 56 (2007) 835.
[2] J. Graetz, S. Chaudhri, Y. Lee, T. Vogt, J. Reilly, Phys. Rev. B 74 (2006), 214114.
[3] J. Graetz, J.J. Reilly, V.A. Yartys, J.P. Maehlen, B.M. Bulychev, V.E. Antonov, B.P. Tarasov, I.E. Gabis, J. Alloys Compd. 509 (2010) S517.
[4] B. Baranowski, M. Tkacz, Z. Phys. Chem. 27 (1983) 135.
[5] S. Kato, M. Bielmann, K. Ikeda, S.-i. Orimo, A. Borgschulte, A. Züttel, Appl. Phys. Lett. 96 (2010), 051912.
[6] Graetz, J.J. Reilly, J. Alloys Compd. 424 (2006) 262,.
[7] T.N. Dymova, D.P. Aleksandrov, V.N. Konoplev, T.A. Silina, N.T. Kuznetsov, Koord. Khim. 19 (1993) 529.
[8] T.N. Dymova, D.P. Aleksandrov, V.N. Konoplev, T.A. Silina, A.S. Sizareva, Koord. Khim. 20 (1994) 279.
[9] P. Claudy, B. Bonnetot, J.M. Letoffe, J. Therm. Anal. 15 (1979) 119.
[10] J.J. Vajo, T.T. Salguero, A.F. Gross, S.L. Skeith, G.L. Olson, Thermodynamic destabilization and reaction kinetics in light metal hydride systems, J. Alloys Compds 446–447 (2007) 409–414, https://doi.org/10.1016/j.jallcom.2007.02.080.
[11] J.J. Vajo, G.L. Olson, Hydrogen storage in destabilized systems, Scripta Mater. 56 (2007) 829–834, https://doi.org/10.1016/j.scriptamat.2007.01.002.
[12] J.J. Vajo, F. Mertens, C.C. Ahn, R.C. Bowman Jr., B. Fultz, Altering hydrogen storage properties by hydride destabilization through alloy formation: LiH and MgH2 destabilized with Si, J. Phys. Chem. B 37 (2004) 13977–13983, https://doi.org/10.1021/jp040060h.
[13] B. Bogdanovic, U. Eberle, M. Felderhoff, F. Schulth, Complex aluminum hydrides, Scripta Mater. 56 (2007) 813–816, https://doi.org/10.1016/j.scriptamat.2007.01.004.
[14] F.M. Brower, N.E. Matzek, P.F. Reigler, H.W. Rinn, C.B. Roberts, D.L. Schmidt, J.A. Snover, K. Terada, J. Am. Chem. Soc. 98 (1976) 2450.
[15] https://www.youtube.com/watch?v=kyT1FQtQAIA.
[16] P.J. Herley, O. Chrlstofferson, R. Irwin, J. Phys. Chem. 85 (1981) 1874.
[17] J. Graetz, J. Reilly, J. Phys. Chem. B 109 (2005) 22181.
[18] B.T. Tang, M.M. Chaudhri, J. Therm. Anal. 17 (1979) 359.